Characterizing Nonrigid Aggregated Soil–Water Medium Using its Shrinkage Curve

Erik Braudeau,* Jean-Pierre Frangi, and Rabi H. Mohtar

ABSTRACT

The properties of the soil–water medium are presented in the literature independent of its internal organization and operation. The objective of this study is to develop and test a conceptual model that used a continuously measured shrinkage curve (SC) to describe the functional organization of the soil–water medium. In this model, two functional porosities (micro and macro) are delineated and quantified by the SC. In addition, the equilibrium for four functional water pools is represented and parameterized by the SC. A set of eleven parameters was found necessary to model the seven phases of the SC and to describe the corresponding soil hydrostructural changes. A method to accurately obtain the parameters of this model by a specific analysis of the continuously measured SC is demonstrated. Examples of continuously measured and modeled SCs according to the pedostructure model (PS) are presented and discussed.

Modeling the SC can be classified in three categories: 1. Those considering certain parts of the curve only such as the model of McGarry and Malafant (1987) and that of Giraldez et al. (1983), which amounts to neglecting or fixing a certain number of parameters; 2. Those modeling its mathematical shape as in the case of Groenevelt and Grant (2001), where they used the sigmoid curve. A limited number of parameters are then necessary (two or three), but the selected parameters do not have any relevance to the processes being modeled; and 3. Those considering the entire SC but making assumptions on the shape of the phases, as is the case of the models of Tariq and Durnford (1993) and Braudeau et al. (1999): a straight line for the quasi-linear parts, and polynomial or exponential function for the curvilinear parts. The parameters of the models are, therefore, representative points of the SC and, contrary to the preceding case, are in connection with the process being analyzed. These points represent particular hydrostructural (see Appendix 1 for definitions) states of the soil and constitute the boundary conditions (V, W) for each shrinkage phase. However, these models do not provide any explanation for the corresponding configuration of the distribution of air, water, and solids in soil, which remains to be explained. The PS proposed in this paper addresses this issue by modeling the entire SC without any embodied assumptions related to its shape and functionality.

E. Braudeau, Institut de Recherche pour le Développement (IRD), Centre de Montpellier, 911 av. Agropolis, BP64501, 34094 Montpellier, France; J.-P. Frangi, Laboratoire Environnement et Développement (LED), Université Paris VII, 2 place Jussieu, BP7071, 75251 Paris Cedex 5, France; R.H. Mohtar, Agricultural and Biological Engineering Dep., Purdue Univ., West Lafayette, IN 47906, USA. Received 23 Nov. 2002. *Corresponding author (erik.braudeau@ird.fr).

Published in Soil Sci. Soc. Am. J. 68:359–370 (2004).

677 S. Segoe Rd., Madison, WI 53711 USA

Braudeau et al. (1999) developed a method for continuously measured SCs providing accurate estimate of the soil water content at each transition point of the shrinkage phases. They recognized seven shrinkage phases on a typical curve (Fig. 1), successively linear and curvilinear, and divided into four stages: interpedal, structural, basic, and residual. They suggested that the transition points (A, B, C, D, E, and F of Fig. 1) are characteristic of the hydrostructural behavior of the soil and they supplied a method to determine these points from soil volume change data using optimal fitting techniques. Appendix 2 describes the equations used by their model. However, these equations were empirically established and thus do not supply any information about the hydrostructural processes of the observed shrinkage phases of the curve; neither do they allow a better understanding of the mechanical, agronomic, and hydraulic properties associated with these shrinkage phases. To quantitatively characterize these properties, we need a physically based equation of the soil SC that is an equation linked to a conceptual model of the soil structure and water interaction.

The nested soil structure has led morphologists to recognize the soil horizon as the basic typological entity composed of peds or aggregates, arranged in several structural levels (Brewer, 1964). The soil and water interactions act at these small scales and are the agents of soil physical properties that emerge at the macroscopic scale. When water is lost from a moist soil core sample, the sample experiences several mechanical states known as shrinkage phases (Yong and Warkentin, 1966). A few studies modeled the hydrostructural changes of soil samples during their shrinkage (Braudeau, 1988a, 1988b; Perrier et al., 1995; Voltz and Cabidoche, 1995; Chertkov, 2000), each using different hypotheses to represent the soil medium.

Two major approaches exist for modeling soil water physical properties in soil matrix. The first views soil structure as an assembly of capillary tubes between and within rigid aggregates, forming only one or two levels of structure. Soil structure is then characterized by a mono- or bimodal distribution of pore volume by class size of equivalent pore diameter (Coppola, 2000). The second approach considers soil structure as an arrangement of particles and swelling aggregates at various scales: clayey plasma, primary peds and assembly of primary peds that constitutes the soil fabric at the hori-

Abbreviations: CARHYS, software for soil hydrostructural characterization; PS, pedostructure (model of shrinkage curve); SC, shrinkage curve; SL, straight lines (method of shrinkage curve parameters determination); XP, exponential (model of shrinkage curve).

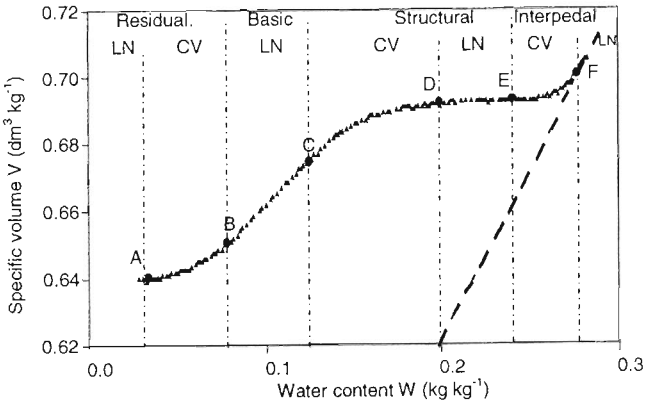

Fig. 1. A typical continuously measured shrinkage curve (SC) of a reconstructed soil sample using three hundred points of measurement. Points A, B, C, D, E, and F are the transition points of the shrinkage phases as determined by parametric modeling of the SC according to the exponential model (XP) of Braudeau et al. (1999). LN, CV refers to as linear and curvilinear phases, respectively.

zon level (Braudeau, 1988a, 1988b; Colleuille and Braudeau, 1996). Figure 2 schematizes this approach and defines the pedostructure as the soil–water fabric of a soil horizon.

The first point of view is the oldest and most widely spread. Many equations arise from it, including the well-known expression relating soil water potential to pore diameter. However, this approach greatly restricts reality because it disregards both the hierarchy of soil structure and the specific properties of the water–plasma interaction such as swelling shrinkage, rearrangement of particles, and the presence of swelling pressure. The second approach recognizes the organized soil structure and the swelling properties of aggregates. Its use has been limited in modeling physical properties even though it better explains and fits observed data. A major obstacle limiting the use of this approach is without a doubt the lack of a recognized experimental method to characterize soil structure scales and their respective contributions to soil hydraulic properties. This requires a method that conceptually distinguishes and delimits the nested

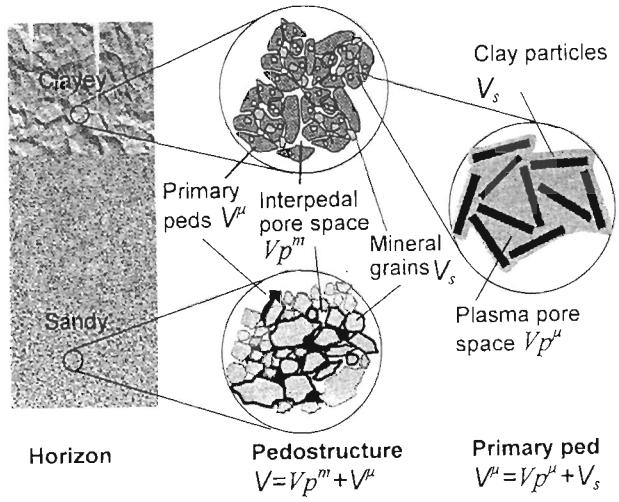

Fig. 2. The pedostructure concept is shown taking into consideration the hierarchical functional levels of the soil medium.

levels of soil structure as well as physically separates these functional levels. Colleuille and Braudeau (1996) proposed a method of soil fractionation into primary aggregates. The basic concept used for the distinction of the primary peds structure level, and thus for the fractionation method, was related to the "air entry point into the soil clayey plasma" (Groenevelt and Bolt, 1972; Sposito, 1973; Sposito and Giraldez, 1976). By definition the primary peds are those representing the first partitioning level of the clayey plasma (Brewer, 1964). At moisture state just before air entry in the plasma, the interpedal porosity is dry while primary peds remain saturated, that defines their functional partitioning. Braudeau (1988a, 1988b) and Braudeau and Bruand (1993) have shown that this air entry point that is the transition point between the basic and the residual shrinkage phases (Point B, Fig. 1) can be obtained precisely from the SC on condition that it is continuously measured. Braudeau et al. (1999) developed a device and a modeling method of the SC to precisely determine the air entry point in the plasma of the soil corresponding to Point B of the SC.

The objective of this study is to develop and test a physically based model of the pedostructure fitting the continuously measured SC during drying. The goal is to characterize and parameterize the soil–water medium using its measured SC to model its internal hydrostructural configuration.

We divide the article into two parts; (i) description of the shrinkage processes and their relationships caused by the removal of the water pools held by each of the two pore systems, inter and intra primary peds, and (ii) application of the PS to the characterization of four soil types.

THEORY

The Different Water Pools in the Pedostructure

For interpreting the SC we define two pools of water in the two pore systems, inside and outside primary peds: swelling water, w_{sw}, and condensed water or nonswelling, w_{cn}. Swelling water occupies a pore space acquired by the spacing of particles or aggregates under the effect of osmotic pressure. Its removal from the sample causes shrinkage of the concerned pore system. Condensed water, on the other hand, occupies an interstitial pore space and is replaced by air (or water vapor at saturation pressure) when it leaves the pore; its loss causes little or no shrinkage. During drying, each linear phase of the SC is caused by the predominant departure of only one pool of water, w_{sw} or w_{cn}, from either the micro- or the macropore system (Fig. 3). The curvilinear components of the SC, which constitute a transition between the two adjacent linear phases, are caused by the simultaneous departure of the two water pools (w_{sw} and w_{cn}) corresponding to these two linear phases. Table 1 shows the different water pools acting in each of the shrinkage phases. The basic relationship between the pedostructure volume change dV and water pools can be written as follows:

$$dV = K_{re}dw_{re} + K_{bs}dw_{bs} + K_{st}dw_{st} + K_{ip}dw_{ip} \quad [1]$$

where K_{re}, K_{bs}, K_{st}, and K_{ip} are slopes of the linear phases (residual, basic, structural, and interpedal) of the SC that are considered constant for the entire range of the water content.

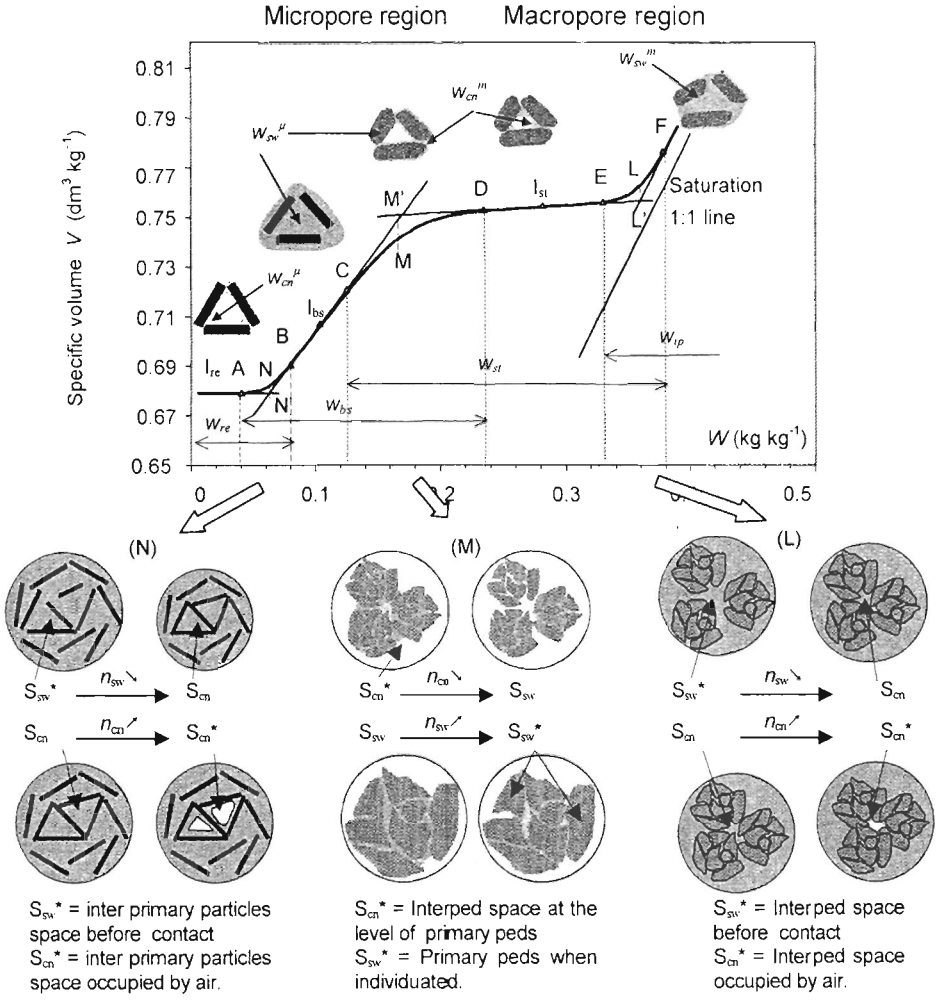

Fig. 3. Various configurations of air and water partitioning into the two pore systems, inter and intra primary peds, related to the shrinkage phases of a standard shrinkage curve (SC). w_{cn} represents the condensed water lodged in interstitial pore site S_{cn}, and w_{sw} represents the swelling water lodged in interstitial pore site S_{sw} that can be interped macropores (^{m}) or matrix micropores ($^\mu$). Asterisk means that the site is active and the corresponding numbers of the active sites are n_{sw} and n_{cn}. The various pools of water, w_{re}, w_{bs}, w_{st}, w_{ip}, are represented with their domain of variation. The inflection points I_{bs} and I_{st}, and by extension I_{re} and I_{ip}, are placed on the graph for representing the quasi-linear shrinkage phases delimited by the transition points (A, B, C, D, E, and F). Points N′, M′, and L′ are the intersection points of the tangents at those linear phases and Points N, M, and L, the corresponding points of the SC.

The water pools within the pedostructure are defined as follows:

w_{re} ($\equiv w_{cn}^{\mu}$) such that $dw_{re} \approx dW$ in the linear residual phase (I_{re});

w_{bs} ($\equiv w_{sw}^{\mu}$) such that $dw_{bs} \approx dW$ in the basic phase (I_{bs});

w_{st} ($\equiv w_{cn}^{m}$) such that $dw_{st} \approx dW$ in the linear structural phase (I_{st}); and

w_{ip} ($\equiv w_{sw}^{m}$) such that $dw_{ip} \approx dW$ in the interpedal phase $W > W_F$.

All the water pools (w_{re}, w_{bs}, w_{st}, w_{ip}) and W, total water

Table 1. Nomenclature and symbols used in the definitions of the various shrinkage phases and the various water pools.

Shrinkage phases†	Residual		Basic	Structural		Interpedal	
	Linear (I_{re})	Curvilinear (N)	Linear (I_{bs})	Curvilinear (M)	Linear (I_{st})	Curvilinear (L)	Linear (I_{ip})
Transition points	A		B	C	D	E	F
Pore system involved	micro (μ) Vp^{μ}	micro (μ) Vp^{μ}	micro (μ) Vp^{μ}	(μ) + (m) $Vp^{\mu} + Vp_m$	macro (m) Vp^{m}	macro (m) Vp^{m}	macro (m) Vp^{m}
Type of water evaporating	Condensed water w_{cn}^{μ}	$w_{cn}^{\mu} + w_{sw}^{\mu}$	Swelling water w_{sw}^{μ}	$w_{sw}^{\mu} + w_{cn}^{m}$	Condensed water w_{cn}^{m}	$w_{cn}^{m} + w_{sw}^{m}$	Swelling water w_{sw}^{m}
Corresponding water pools‡	w_{re}	$w_{re} + w_{bs}$	w_{bs}	$w_{bs} + w_{st}$	w_{st}	$w_{st} + w_{ip}$	w_{ip}

† I_{re}, I_{bs}, I_{st}, I_{ip}, and N, M, L, are points of the shrinkage curve used to represent a shrinkage phase (see Fig. 3).
‡ w_{re}, w_{bs}, w_{st}, and w_{ip} are the four water pools corresponding to condensed or swelling water held in the micro– and macropore systems of the pedostructure. They decrease and vanish successively with decreasing water content from the soil sample.

content of the sample, are expressed as mass of water divided by mass of dry soil (kg kg^{-1}); thus the relationship between the different water pools of the pedostructure is:

$$W = w_{re} + w_{bs} + w_{st} + w_{ip} \quad [2]$$

The constants K_{re} and K_{st} are near zero and much smaller than K_{bs} and K_{ip}. The above definitions and assumption, and definition of the specific volumes in Fig. 2, makes it possible to quantitatively represent the volume change of the different elements of the pedostructure in terms of the main SC variables, V and W (Fig. 4).

Following is a derivation of each of the water pools that constitute the components of Eq. [1].

Let us consider the curvilinear parts of the SC, J (J = L, M, N), located between the inflection points of two adjacent linear phases: L for (I_{ip} and I_{st}), M for (I_{st} and I_{bs}) and N for (I_{bs} and I_{re}) (Fig. 3). According to Table 1, each Segment J is associated with a swelling (of micro or macropore) and condensed (of micro or macropore) water pair such as (w_{sw}^{m} and w_{cn}^{m})^{L}, (w_{cn}^{m} and w_{sw}^{μ})^{M}, and (w_{sw}^{μ} and w_{cn}^{μ})^{N} for J = L, M and N, respectively. Let Π_{sw}^{J} (or Π_{cn}^{J}) be the probability of water pool pair w_{sw} (or w_{cn}) that is lost from the sample during drying at a given water content of Region J, then:

$$\Pi_{sw}^{J} = \frac{dw_{sw}}{dw_{sw} + dw_{cn}}; \quad \Pi_{cn}^{J} = \frac{dw_{cn}}{dw_{sw} + dw_{cn}}$$
$$\text{where } \Pi_{sw}^{J} + \Pi_{cn}^{J} = 1 \quad [3]$$

where w_{sw} can be replaced by w_{bs} or w_{ip}, and w_{cn} by w_{re} or w_{st} depending on the stage of J (N, M, or L; Table 1). In fact, Π_{cn}^{J} and Π_{sw}^{J} represent the respective fractions of the two water pools of the SC Region J, available for evaporation at the water content W. These two fractions can be considered at the same energy level depending on W assuming that evaporation is sufficiently slow so that the SC can be regarded as a succession of equilibrium states after each change of water content dW.

Each water pool is in interstitial sites S_{sw} or S_{cn} (of swelling or nonswelling) that can be active or not as defined in Fig. 3. Let n_{sw} and n_{cn} be the numbers of active sites of swelling and condensed at J. It is assumed that, for a variation of water content dW, the number dn_{sw} (or dn_{cn}) of active sites which appear for one water pool and disappear for the other (Fig. 3), is proportional to dW and to the number of active sites n_{sw} (or n_{cn}) present such that:

$$dn_{sw}/dW = kn_{sw} \text{ and } dn_{cn}/dW = k'n_{cn} \quad [4]$$

This amounts to assuming an exponential progression of the number of active sites with water lost during drying, increasing for one water pool and decreasing for the other:

$$n_{sw} \sim A^{W} \text{ and } n_{cn} \sim B^{W} \quad [5]$$

Since, for the shrinkage Region J, the loss of a water pool is proportional to the number of its active sites, the probability Π_{sw}^{J} can be expressed as:

$$\Pi_{sw}^{J} = \frac{dw_{sw}}{dw_{sw} + dw_{cn}} = \frac{n_{sw}}{n_{sw} + n_{cn}} = \frac{aA^{W}}{aA^{W} + bB^{W}}$$
$$= \frac{(a/b)(A/B)^{W}}{1 + (a/b)(A/B)^{W}}$$

which can be written as:

$$\Pi_{sw}^{J} = \frac{\exp[k_J(W - W_J)]}{1 + \exp[k_J(W - W_J)]} \text{ and}$$
$$\Pi_{cn}^{J} = \frac{1}{1 + \exp[k_J(W - W_J)]}. \quad [6]$$

where a, b, A, B are constants, k_J is a constant characteristic of segment J (= N, M, or L) of the SC, and W_J is the water content at Point J (= N, M, or L) of this segment such as $\Pi_{sw}^{J} = \Pi_{cn}^{J} = 1/2$. Integration of Eq. [6] between 0 and W gives:

$$w_{sw} = \frac{1}{k_J}\text{Log}\left\{\frac{1 + \exp[k_J(W - W_J)]}{1 + \exp(-k_J W_J)}\right\} \text{ and}$$
$$w_{cn} = \frac{1}{k_J}\text{Log}\left\{\frac{1 + \exp[-k_J(W - W_J)]}{1 + \exp(k_J W_J)}\right\} \quad [7]$$

In Region L of the SC, d$W \approx$ dw_{ip} + dw_{st}, and

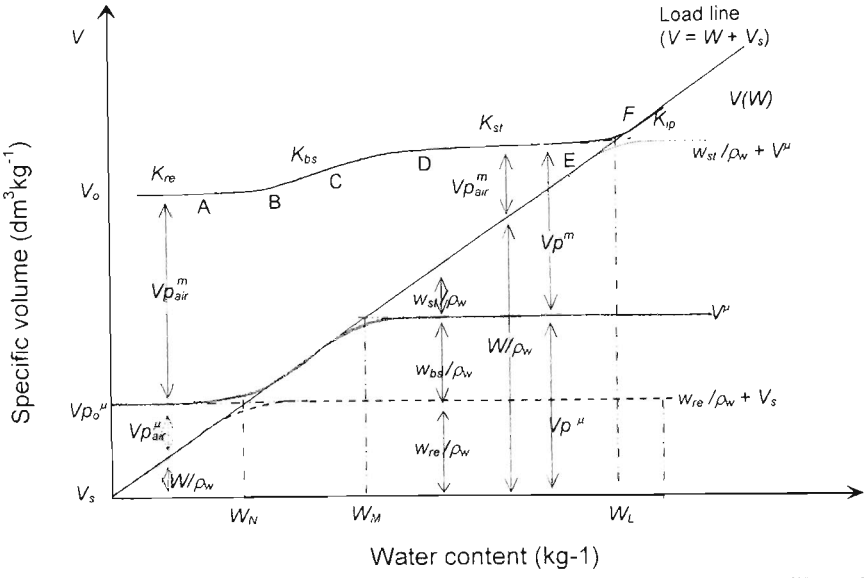

Fig. 4. Graphical representation of the specific volumes (V^{μ} and V), the specific pore volumes (Vp^{μ} and Vp^{m}), the air contents (Vp_{air}^{μ} and Vp_{air}^{m}) and the water pools (W, w_{re}, w_{bs}, w_{st}, and w_{ip}) of the pedostructure starting from a measured SC. V^{μ} is the specific volume of primary peds, equal to ($Vp^{\mu} + V_s$) = [max (w_{re})ρ_w + w_{bs} ρ_w + V_s], and ρ_w is the water bulk density.

Table 2. Values of the probabilities Π^J_{sw} and $\Pi^J_{cn} = 1 - \Pi^J_{sw}$ in the different shrinkage phases during drying for each water pool. The subscript sw correspond to the swelling water pool (w_{ip} or w_{bs}) and cn to the condensed water pool or nonswelling (w_{st} or w_{re}) of the same pair associated with Region J of the shrinkage curve (SC).

Shrinkage phases	Π^N_{re}	Π^N_{bs}	Π^M_{bs}	Π^M_{st}	Π^L_{st}	Π^L_{ip}
(I_{ip})	0	1	0	1	0	1
(L)					$0 < \Pi < 1$	$1 > \Pi > 0$
(I_{st})	0	1	0	1	1	0
(M)			$0 < \Pi < 1$	$1 > \Pi > 0$		
(I_{bs})	0	1	1	0	1	0
(N)	$0 < \Pi < 1$	$1 > \Pi > 0$				
(I_{re})	1	0	1	0	1	0

$$\Pi^L_{sw} = \Pi^L_{ip} = \frac{\exp[k_L(W - W_L)]}{1 + \exp[k_L(W - W_L)]},$$

$$\Pi^L_{cn} = \Pi^L_{st} = \frac{1}{1 + \exp[k_L(W - W_L)]} \quad [8]$$

with $k_L > 0$ since for $W \gg W_L$, $\Pi_{ip} \approx 1$ and $\Pi_{st} \approx 0$; and for $W \ll W_L$, $\Pi_{ip} \approx 0$ and $\Pi_{st} \approx 1$.

In Region M, $dW \approx dw_{bs} + dw_{st}$ and:

$$\Pi^M_{bs} = \frac{\exp[k_M(W - W_M)]}{1 + \exp[k_M(W - W_M)]} \text{ and}$$

$$\Pi^M_{st} = \frac{1}{1 + \exp[k_M(W - W_M)]} \text{ where } k_M < 0 \quad [9]$$

In Region N, $dW = dw_{bs} + dw_{re}$ and

$$\Pi^N_{bs} = \frac{\exp[k_N(W - W_N)]}{1 + \exp[k_N(W - W_N)]} \text{ and}$$

$$\Pi^N_{re} = \frac{1}{1 + \exp[k_N(W - W_N)]} \text{ with } k_N > 0. \quad [10]$$

Each probability Π^J is a logistic equation that varies asymptotically between 0 and 1, as shown in Table 2.

Each water pool above has its own active domain and thus must be considered separately. Equations for the four water pools follow:

(a) For the case of w_{re} that varies only in Segment N of the SC, integrating Eq. [6] where $\Pi^J_{cn} = \Pi^N_{re}$ and considering $\exp(k_N W_N) \gg 1$ gives:

$$w_{re} = \int_0^W \Pi^N_{re} dW = -\frac{1}{k_N} \log\left\{\frac{1 + \exp[-k_N(W - W_N)]}{1 + \exp(k_N W_N)}\right\},$$

which can be written as:

$$w_{re} \approx W_N - \frac{1}{k_N} \log\{1 + \exp[-k_N(W - W_N)]\} \quad [11]$$

(b) For the case of w_{bs}, the variation of w_{bs} occurs in Segments N and M, dw_{ip} can be ignored rather than dw_{re}, dw_{bs}, dw_{st}, therefore, we can write:

$$\frac{dw_{bs}}{dW} = \frac{dw_{bs}}{dw_{re} + dw_{bs} + dw_{st}} \quad [12]$$

The product ($dw_{re}\, dw_{st}$) is negligible and therefore ignored in the following equation:

$$\Pi^M_{bs}\, \Pi^N_{bs} = \frac{dw_{bs}}{dw_{re} + dw_{bs}} \frac{dw_{bs}}{dw_{bs} + dw_{st}} \approx \frac{dw_{bs}}{dw_{re} + dw_{bs} + dw_{st}} \quad [13]$$

Therefore:

$$w_{bs} = \int_0^W 1 \Pi^N_{bs} \Pi^M_{bs} dW \quad [14]$$

Considering the values of Π^J given in Table 2, Eq. [14] can be expressed as:

$$w_{bs} = \int_0^W \Pi^N_{bs}\, dW + \int_{W_{Ibs}}^W \Pi^M_{bs}\, dW - \int_{W_{Ibs}}^W dW \quad [15]$$

where W_{Ibs} is the water content at the inflection point of the basic shrinkage phase.

According to Eq. [7], integration of [15] gives:

$$w_{bs} = \frac{1}{k_N} \log\{1 + \exp[k_N(W - W_N)]\} + \frac{1}{k_M} \log\{1 + \exp[-k_M(W - W_M)]\} \quad [16]$$

One can verify that since $k_N > 0$ and $k_M < 0$, $\max(w_{bs}) \approx (W_M - W_N)$ for $W \gg W_M$.

(c) Similar to the previous case, the case of w_{st}, which varies in Segments M and L of the SC, gives:

$$w_{st} = \int_0^W \Pi^M_{st} \Pi^L_{cn} dW = \int_0^W \Pi^M_{st} dW + \int_{W_{Ist}}^W \Pi^L_{st} dW - \int_{W_{Ist}}^W dW \quad [17]$$

$$w_{st} = -\frac{1}{k_M} \log\{1 + \exp[-k_M(W - W_M)]\} - \frac{1}{k_L} \log\{1 + \exp[k_L(W - W_L)]\} \quad [18]$$

and since $k_L > 0$, $\max(w_{st}) \approx (W_L - W_M)$ for $W \gg W_L$.

d) For the case of w_{ip}, that varies only in Segment L of the SC, according to Eq. [7] where $\Pi^J_{sw} = \Pi^L_{ip}$ and ignoring $\exp(-k_L W_L)$ below 1:

$$w_{ip} = \int_0^W \Pi^L_{sw}\, dW = \frac{1}{k_L} \log\left\{\frac{1 + \exp[k_L(W - W_L)]}{1 + \exp(-k_L W_L)}\right\} \approx \frac{1}{k_L} \log\{1 + \exp[k_L(W - W_L)]\} \quad [19]$$

And

$$w_{ip} \approx (W - W_L) \text{ when } W > W_F \quad [20]$$

Significance and Determination of Water Pools Parameters

According to Eq. [1], the parametric equation of the SC is:

$$V = V_o + K_{re} w_{re} + K_{bs} w_{bs} + K_{st} w_{st} + K_{ip} w_{ip} \quad [21]$$

where V_o is the specific volume of the dry sample. Equation [21] can be considered as the pedostructure variation law in which K_{re}, ..., K_{ip}, are the (geometrical) parameters, and w_{re}, ..., w_{bs}, the parametric functions of water pools at equilibrium

represented by Eq. [11], [16], [18], and [19]. The variation law (Eq. [1]) with its parameters and functions represent the PS in which all of its variables shown in Fig. 4 are at equilibrium defined by the SC.

The physical significance of the six parameters (k_N, k_M, k_L, W_N, W_M, W_L) used in the water pool functions is demonstrated in Appendix 3. The points of the SC for water contents $W_{J\ (J = N, M, L)}$ have the same x-coordinates as the intersection points (N′, M′, and L′) of the tangents to the linear parts of the SC (Fig. 3); and the constants k_J represent the reverse of the vertical (y axis) distance (NN′, MM′, and LL′) between those intersection points and the SC segments ($k_{N,L} > 0$ and $k_M < 0$):

$$W_N = W_{N'};\ W_M = W_{M'};\ W_L = W_{L'};$$
$$k_N = \frac{K_{bs} - K_{re}}{V_{N'} - V_N}\log(2);\ k_M = \frac{K_{bs} - K_{st}}{V_{M'} - V_M}\log(2);$$
$$k_L = \frac{K_{ip} - K_{st}}{V_{L'} - V_L}\log(2) \qquad [22]$$

Using relationships in Eq. [22] the six parameters of the water pools are easily calculated from the continuously measured SC after having drawn the four tangents of the SC at the inflection points.

Comparison with the Exponential Model

The foregoing conceptual PS uses a total of eleven parameters, six for the water pools and five for the structure:

$$k_N, k_M, k_L, W_N, W_M, W_L, K_{re}, K_{bs}, K_{st}, K_{ip}, V_o \qquad [23]$$

The independent parameters of the SC exponential model (XP) proposed by Braudeau et al. (1999) also uses a total of 11 parameters, namely:

$$W_A, W_B, W_C, W_D, W_E, W_F, K_{re}, K_{bs}, K_{st}, K_{ip}, V_A \qquad [24]$$

The method of determining the parameters of the PS using Eq. [22] and the tangents of the SC, is similar to the Straight Lines (SL) method for determining the phase transition Points A, B, ... and F proposed by Braudeau et al. (1999) for the XP model. This method draws the four tangents to the SC and uses the vertical distances between the points N′, M′, L′, and their homologs N, M, L on the SC (Fig. 3) to determine the position of the transition phases using the relationships shown in Table 3 such as:

$$(K_{bs} - K_{st})/(V_{M'} - V_M = 4.8/(W_M - W_D) = 3.46/(W_C - W_M) \qquad [25]$$

and

$$(V_C - V_D)/(W_C - W_D) = (0.718\ K_{bs} + K_{st})/1.718 \qquad [26]$$

Points A, B, ..., and F are specific to the XP and do not physically exist according to the PS. The water pools equations (Eq. [11], [16], [18], and [19]) are asymptotic and there is no clear transition from one phase to another, as in the XP where one passes from an exponential curvilinear to a linear phase. From the point of view of the PS, the location of Points A, B, ..., and F is an empirical approximation to mark a change in the effective state of pedostructure where the two pore systems are in one of three swelling states: minimum, variable, or maximum; and one of three saturation states: empty, unsaturated, and saturated. Thus, according to Fig. 3 showing the behavior of each water pool on the SC with decreasing water content, the transition points of the XP model can be considered as approximations of particular hydral states as follows: Point F like the interpedal (macropore) air-entry; Point E, the interpedal shrinkage limit; Point D, the primary peds shrinkage beginning; Point C, the dry macropore point; Point B, the micropore air-entry; and Point A, the shrinkage limit.

Using the Shrinkage Curve for Soil Characterization

As shown above, parameter lists [23] and [24], can be easily estimated from the measured SC using the SL method (Braudeau et al., 1999). An optimization algorithm was implemented to fit the data to the above equations using the simplex method. Accordingly, W_N, W_M, W_L characterizes the pore systems using the water pools definition, such as:

$$\min(Vp^{\mu}) = W_N/\rho_w;\ \max(Vp^{\mu}) = W_M/\rho_w;$$
$$Vp_F = W_L \qquad [27]$$

where ρ_w is the water bulk density.

A special case occurs where the PS and XP act differently. This is the case of very swelling soils where the macroporosity of the pedostructure is not significant and the polyhedral aggregates are assembled by their microsurfaces. The structural shrinkage phase (E-D) is reduced and may even not exist so the I_{ip} and I_{bs} shrinkage phases (Table 1) are overlapping. In addition, the primary peds begin to retract before all the aggregates are in complete contact (at Point E) giving $W_D > W_E$. In this case and for the PS model, K_{st} must be taken as equal to zero and should not be confused with the slope of the shrinkage Phase E–D as it was done with the XP (Braudeau et al., 1999).

MATERIALS AND METHODS

The soil samples used in this study came from two sources:

1. A pedological cartography and characterization of an irrigated area in the lower valley of Majerda, 20 km north of Tunis (North Tunisia), on recent deltaic alluvia near the Mediterranean Sea. This study (Braudeau et al., 2001) was undertaken within the framework of a development project with emphasis on pedological information system where the physical soil characterization was to be based on the retractometric analysis. Shrinkage curves were measured and analyzed on recast soil cores. The SC measurements were made by means of a "retractometer" (Braudeau et al., 1999). Soil samples were gently disaggregated and 2-mm sieved, then reconstructed in consistent cylinders by piling up the aggregates in a 5.5-cm diameter and 4.0-cm long PVC cylinder and packing down the cylinders by one cycle of moistening–drying under free air and stress conditions (Zidi and Braudeau, 1998). The SC measurements constitute 400

Table 3. Relationships between pedostructure model (PS) and exponential model (XP) shrinkage curve parameters via the tangents intersection points (L′, N′, M′) of the Straight Lines (SL) method of Braudeau et al. (1999).

Shrinkage phases concerned	PS - SL - XP relationships
Basic and residual (N)	$k_N/\ln(2) = (K_{bs} - K_{re})/(V_N - V_{N'}) = 4.8/(W_N - W_A) = 3.46/(W_B - W_N)$
Basic and structural (M)	$k_M/\ln(2) = (K_{bs} - K_{st})/(V_M - V_{M'}) = 4.8/(W_M - W_D) = 3.46/(W_C - W_M)$
Interpedal and structural (L)	$k_L/\ln(2) = (K_{ip} - K_{st})/(V_L - V_{L'}) = 4.8/(W_L - W_E) = 3.46/(W_F - W_L)$

to 800 points, equivalent to one data point per minute. Three of the SCs from their study will be used in this paper: one for a soil located in an old raised bank with loam texture and the other in the decantation plain with clay-loam texture. Their great group name in Soil Taxonomy Survey (Soil Survey staff, 1996) is Xerofluvents. They are referred to as Alluvial 1, 2, and 3 in Table 4 and Fig. 5.

2. Four soils, all in Senegal, studied by Braudeau et al. (1999). Their great group names are Pellustert, Torrifluvents, Plinthustox, and Plinthustalf. Soil samples were reconstituted with <2-mm sieved aggregates in consistent cylinders (diameter 55 mm; height 35 mm). After their wetting on a porous ceramic plate (12 h) they were equilibrated (48 h) at a matrix potential of −100 kPa before they were smoothly compacted under a given pressure to reach the specific volume of the undisturbed soil. Unlike the precedent study above, the SC data files are not available and only the XP parameters of the last five shrinkage phases of the SC (eight parameters) are provided. Parameters were determined by minimizing the difference between the XP and the measured SC. Two clayey soils were taken as examples in this work for comparison between the PS model and the XP: the Pellustert and the Plinthustox referred to in tables and figures as Vertisol and ferrallitic soil. Their SC was redrawn according to the equations and parameters of the XP (Braudeau et al., 1999) and was then fitted according to the PS.

The pedohydral parameter estimation procedure consisted of conducting an optimized adjustment of the continuously measured SC to the parametric pedostructure equation of state [21] [$V = f(w_i)$ at constant pressure and temperature]. This process was implemented in computer software for soil hydrostructural characterization (CARHYS) in four steps using the simplex method:

Step 1: Manually estimating the initial location of Points B, C, and D on the measured SC. Points B and C are located inside the linear basic shrinkage phase to determine the parameters of the tangent (of slope K_{bs}) passing through the basic shrinkage phase, which remains constant during the optimization. Point D is placed inside the linear structural shrinkage phase to limit the interval subjected to adjustment in the second step between the Point D and the last measured point of the curve $\{V_D - V_{final}\}$. V_{final} is the specific volume corresponding to the last reading.

Step 2: Adjusting segment $\{V_D - V_{final}\}$ of the measured SC using the following relationship $V1 = V_{N'} + K_{bs}\, w_{bs}$ and considering (i) $K_{re} = 0$ and $V_0 = V_{N'}$, (ii) the tangent to the basic shrinkage phase, of slope K_{bs}, is given (determined using linear regression) and that (iii) W_N, $V_{N'}$, W_M, k_N, k_M are the variable parameters to be determined ($V_{N'}$ is the y-axis coordinate corresponding to W_N on the given tangent).

Step 3: Adjusting the curve ($V_{measured} - V1$) versus W for the whole range of the water content using $V2 = K_{st}\, w_{st} + w_{ip}$ while keeping K_{st}, W_L, and k_L variables with the constraint that the maximum value of K_{st} is fixed at 0.07. Beyond that, K_{st} is taken as zero, considering that the linear phase of this structural shrinkage is missing and that an overlap exists between the two curvilinear Phases M and N caused by w_{bs} and w_{ip} water pools.

Step 4: Adjusting the whole SC using $V = V_0 + K_{bs}\, w_{bs} + K_{st}\, w_{st} + w_{ip}$ considering only W_M, k_M, W_L, and k_L as variable parameters.

The above procedure is repeated for various initial conditions to ensure global optimal solution is reached.

The optimization procedure used to determine these PS parameters at each step is based on the simplex algorithm. The final adjustment evaluated by the mean square deviation

Table 4. Results of the shrinkage curve (SC) parameters for the examples in Fig. 5 and 6 using software for soil hydrostructural characterization (CARHYS). Means and standard deviations (SD) are calculated for 12 CARHYS runs for each sample. Data in italics are the given pedohydral parameters data of Braudeau et al. (1999).

	PS modeling (CARHYS)				XP modeling		PS modeling (CARHYS)			
							Ferralitic (19 × 21)		Vertisol (43 × 14)	
Parameters of the XP and PS models†	Alluvial1 (2 × 15)‡ Mean	Alluvial2 (27 × 27) Mean	Alluvial3 (35 × 50) Mean	Maximal SD	Ferralitic (19 × 21)	Vertisol (43 × 14)	Mean	SD	Mean	SD
				XP model parameters						
W_A	0.027	0.038	0.044	3×10^{-3}	*0.097*	*0.073*	0.097	9×10^{-4}	0.073	3×10^{-4}
W_B	0.079	0.089	0.135	4×10^{-3}	*0.110*	*0.106*	0.109	8×10^{-4}	0.105	4×10^{-4}
W_C	0.128	0.183	0.236	5×10^{-3}	*0.120*	*0.195*	0.122	2×10^{-3}	0.207	5×10^{-4}
W_D	0.197	0.282	0.370	4×10^{-3}	*0.155*	*0.276*	0.163	5×10^{-3}	0.323	2×10^{-3}
W_E	0.246	0.276	0.375	3×10^{-3}	§	§	0.296	3×10^{-3}	0.242	5×10^{-4}
W_{sat}	0.274	0.316	0.414	3×10^{-4}	*0.344*	*0.321*	0.341	2×10^{-3}	0.323	3×10^{-4}
V_A	0.640	0.583	0.598	3×10^{-4}	*0.707*	*0.536*	0.707		0.536	
				Common XP and PS parameters						
K_{re}	0	0	0		*0*	*0.10*	0	0	0	0
K_{bs}	0.52	0.74	1.13	2×10^{-2}	*0.66*	*0.84*	0.610	8×10^{-3}	0.84	2×10^{-3}
K_{st}	0.008	0.004	0.023	3×10^{-3}	*0.034*	*0.428*	0.018	7×10^{-3}	0.000	0
K_{ip}	1	1	1		*1*	*1*	1		1	
				PS model parameters						
k_N	110	114	63	5	426	174	476	60	180.7	4
k_M	−83	−58	−42	3	−166	−71	−140	17	−49.3	0.7
k_L	114	81	84	6	80¶	80¶	75	2	54.6	0.2
W_N	0.057	0.067	0.097	2×10^{-3}	0.105	0.092	0.104	2×10^{-4}	0.092	1×10^{-4}
W_M	0.157	0.224	0.292	2×10^{-3}	0.135	0.229	0.139	1×10^{-3}	0.255	4×10^{-4}
W_L	0.274	0.316	0.414	3×10^{-4}	0.344	0.321	0.341	2×10^{-3}	0.303	3×10^{-4}
$V_{N'}$	0.640	0.583	0.598	3×10^{-4}	0.707	0.536	0.707		0.536	

† PS, pedostructure; XP, exponential.
‡ (Clay% × silt < 50 μm%).
§ Values of W_E were not given.
¶ Values that could not be determined from the initial set of parameters (W_E missing); they were arbitrarily chosen.

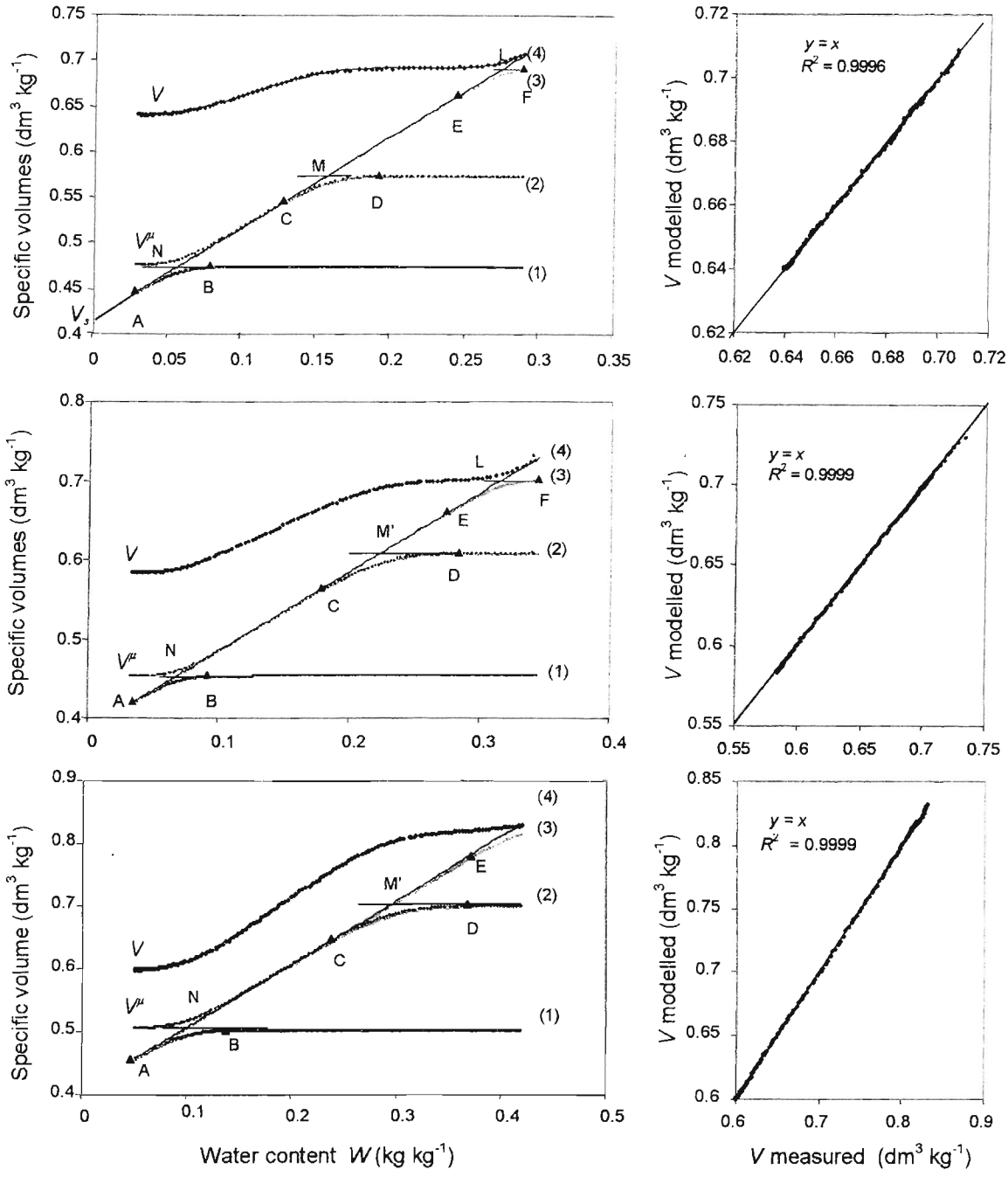

Fig. 5. Continuously measured and modeled shrinkage curves (SCs) for three alluvial soils in the Lower Majerda Valley, Tunisia, using the retractometry procedure. The graph on the right hand side shows the fit for the whole data range. One out of three points is represented. The parameters determined by software for soil hydrostructural characterization (CARHYS) are shown in Table 4. The cumulative variation curves of the water pools, w_{re}, w_{bs}, w_{st}, and w_{ip}, added to V_s are represented referring to as (1), (2), (3), and (4), respectively. Points A, B, C, D, E, and F are the transition points of the shrinkage phases defined by the exponential model (XP) and represented on the corresponding water pools curves.

between the measured and the PS-modeled SC is around 10^{-6}, 10^{-7}. The output of CARHYS is a file containing the resulting parameters of the PS, and also those of the XP that are deducted from the PS parameters using the relationships shown in Table 3.

RESULTS AND DISCUSSION

Figure 5 shows the measured and PS-based modeled SCs of the three alluvial soils of Tunisia along with the changes in water pools and in specific micro- and macropore volumes calculated using the PS. In the three examples, the measured and modeled SCs cannot be distinguished, the mean deviation being 3.6×10^{-4}, 3.8×10^{-4}, and 7.0×10^{-4} dm^3 kg^{-1} for the three soils with a coefficient of correlation >0.9995. The two sets of parameters (PS and XP) determined by CARHYS for these soils are shown in Table 4. Results are presented as means and standard deviations of the parameters

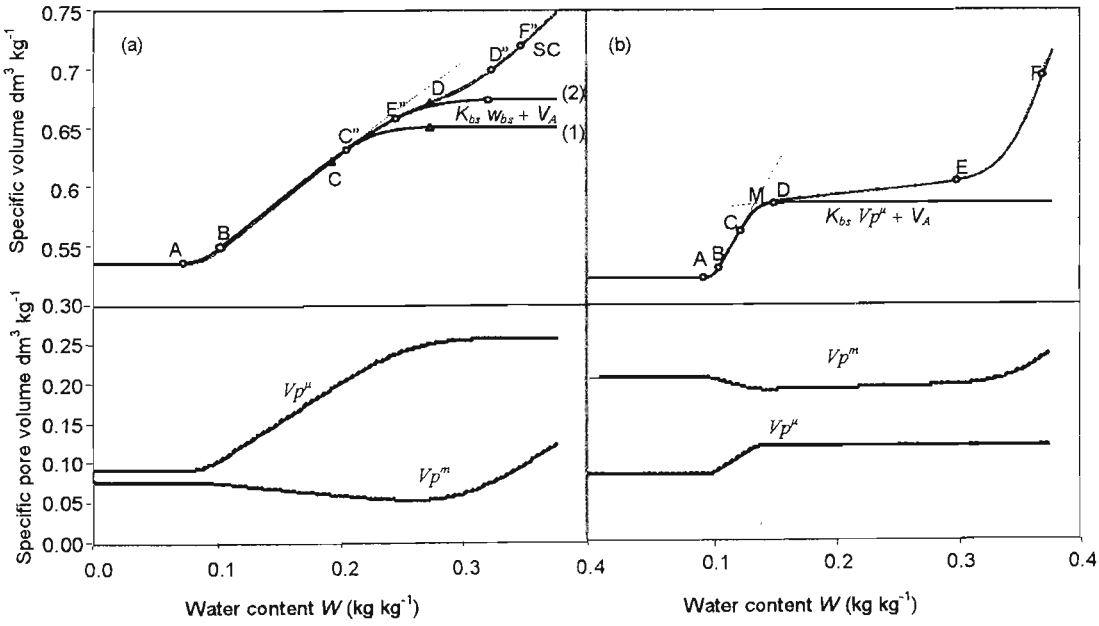

Fig. 6. Shrinkage curves (SCs) and the corresponding micro and macropore volume (Vp^{μ} and Vp^{m}) of two clayey soils in Senegal: (a) vertisol, and (b) ferralitic soil. For the swelling soil case (Fig. 6a) Curve 1 is the modeled w_{bs} water pool contribution ($K_{bs}w_{bs} + V_A$) to the SC when $K_{st} = 0.4$ and Curve 2 when $K_{st} = 0$. (Points A, B, C, and D are the initial parameters determined by the exponential model (XP) with taking $K_{st} = 0.4$; Points C″, D″, E″, and F″ were obtained by CARHYS using the pedostructure (model for SCs) model with $K_{st} = 0$).

using CARHYS analysis for twelve different initial locations of the transition points. It can be seen that the robustness of the CARHYS procedure based on the PS model equations for determining the pedohydral parameters is very good.

Figure 6a and 6b shows a comparison between the XP and PS. The data given by Braudeau et al. (1999) of the two clayey soils from Senegal, vertisol, and ferrallitic soil were used. Equations in Table 3 were used to calculate the PS parameters from the XP parameters (Table 4, Columns 5 and 6) to draw PS SCs. The XP SC were also drawn from the XP parameters. The XP and PS curves represented in Fig. 6a and 6b for the two soils cannot be distinguished. The mean deviation between the PS and XP modeled SC, calculated for 200 points for the interval $\{W_A–W_E\}$, was found to be $<1.5 \times 10^{-4}$ and 0.9×10^{-4} for the vertisol and ferrallitic soil, respectively. However, when CARHYS was used for these SC for determining the pedohydral parameters, they were found to be the same as the values given for the ferrallitic soil and were different for the vertisol (Columns 5 and 6 in Table 4). This is explained by the fact that CARHYS fits the SC using the pedostructure conceptual model that does not accept a value of 0.4 for K_{st}, the slope of the structural shrinkage phase, as determined by the XP. As mentioned above, K_{st} values are often near zero and cannot exceed 0.07. If a higher value of K_{st} is found by the XP procedure (SL method, Braudeau et al., 1999) as in the case of the vertisol (Fig. 6a), the interpedal swelling water pool, w_{ip}, is not completely vanished when the shrinkage of the primary peds starts to be effective. In this case, there is no structural shrinkage phase and K_{st} must be taken as zero.

Figure 6a shows how the particular case of the vertisol was considered by CARHYS and the XP. For this soil the contribution of the swelling water, w_{bs}, calculated using $K_{st} = 0.4$, is lower (Curve 1) than that calculated by using $K_{st} = 0$ (PS, Curve 2). This correction (taking $K_{st} = 0$) shows that the volume change of primary peds was underestimated by the XP, but above all, W_E can be smaller than W_D, signifying that the beginning of the clayey plasma shrinkage takes place before the interped shrinkage limit at Point E.

Figure 6b shows the case for ferrallitic soil, clayey but weakly swelling soil. The structural linear shrinkage phase (E–D) is well discernible with a slope of $K_{st} = 0.034$ dm³ kg^{-1}. CARHYS determined the same values of the parameters as those given by the XP.

The decrease in macropore volume shown in the figure in the range $\{W_F–W_E\}$ is directly related to the decrease in w_{ip}. In the range $\{W_D–W_A\}$, this change is related to the micropore volume decrease, depending on K_{bs} being smaller or greater than unity, according to the following relationships: $dVp^m = (K_{bs} - 1)\, dVp^{\mu}$.

The above results show the entire compatibility of both models. Both fit well the continuous measured SC even though their basic hypotheses and the resulting implications are different (Fig. 7). The PS, more realistically, is based on a conceptual model of the soil fabric in equilibrium with its water pools. It models all the state variables of the pedostructure. On the other hand, the XP is based on partitioning of the SC into linear and exponential segments. It determines an empirical delineation of the shrinkage phases and thus defines phase transition points that are taken as parameters.

Figure 7 shows an example of how the exponential function of the XP (Appendix 3) simulates the curvilinear segment of the curve $w_{bs} = f(W)$ for the vertisol (Eq. [16]), and how it can thus approximate the effective beginning and end of change in curvature, namely Points

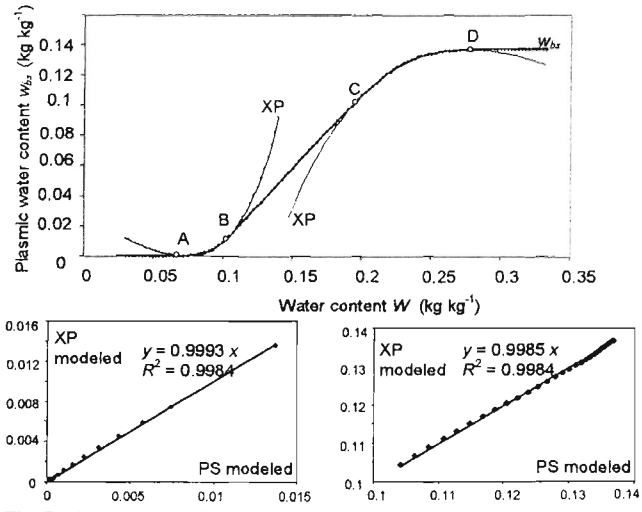

Fig. 7. An example of how the exponential functions of the exponential model (Eq. [A1]) simulates the curvilinear part of the curve $w_{bs} = f(W)$ of the vertisol (Eq. [16]), and how it can thus determine the effective beginning and end of variation of the curve. The mean deviations between the two fitted curves in the ranges {WD–WC} and {WB–WA} are 3.5×10^{-4} and 1.4×10^{-4} dm^3 kg^{-1}, respectively.

A and D, where the derivatives of the XP are zero. This approximation is thus defined by the shape of the empirical parametric function chosen to model the curvilinear parts of the curve (Eq. [A1]). In this sense, the XP is a standardized empirical means of defining the location of soil–water behavior change on the SC.

The pedostructure concept is then composed of the XP model, which defines the change in macroscopic soil physical properties, and the PS model that simulates the internal soil–water medium equilibrium for each water content. Together they describe, internally and externally, the description space of the pedostructure, of which the eigenvalues are the set of parameters [23] or [24] (Appendix 3).

CONCLUSION

This article shows how the SC can be considered and modeled as a result of soil structural variation law and logistic probability functions for coupled water pools (swelling and nonswelling) for micro- and macropore system equilibrium.

As a result, the continuously measured SC can be used as a unique characteristic of the soil–water medium that offers a quantitative description of its internal organization and operation.

A new pedostructure concept was described for characterizing the external and internal behavior of the soil horizon. This new paradigm will have significant implications on modeling and characterizing soil–water dynamics.

APPENDIX 1

List of definitions

Functional scales: levels of scales in the soil medium defined by their soil–water interaction and operation contrary to their classification by size.

Hydrostructural: interaction between soil water and soil structure.

Pedohydral parameters: parameters of the shrinkage curve.

Pedostructure: the soil-water medium of the soil horizon composed of the assembly of peds in several organizational levels, the last of which is that of the primary peds. It refers to the combination of the soil fabric and its dynamic operation with water.

Nomenclature

V, Pedostructure specific volume, dm^3 per kg of dry soil horizon
V^{μ}, Primary peds specific volume, dm^3 per kg of dry soil horizon
V_s, Solids (primary particles) specific volume, dm^3 per kg of dry soil horizon
Vp, Pedostructure pore specific volume, dm^3 per kg of dry soil horizon
Vp^m, Macropore specific volume of pedostructure, dm^3 per kg of dry soil horizon
Vp$^{\mu}$, Micropore specific volume of pedostructure, dm^3 per kg of dry soil horizon
W, Pedostructure water content (soil moisture), kg per kg of dry soil horizon
w_{rs}, Pedostructure residual water pool, kg per kg of dry soil horizon
w_{bs}, Pedostructure basic water pool, kg per kg of dry soil horizon
w_{ss}, Pedostructure structural water pool, kg per kg of dry soil horizon
w_{ip}, Pedostructure interpedal water pool, kg per kg of dry soil horizon
A, B, C, D, E, F, Shrinkage transition points of the SC defined by the XP model
N′, M′, L′, Intersection points of the tangents to the SC at the linear phases
N, M, L, Characteristic points of the SC at the vertical (y axis) of N′, M′, L′
I_{ss}, I_{bs}, Inflection points of structural and basic shrinkage phases
W_A, W_B, ... W_F, Pedostructure water content (kg kg^{-1}) at Points A, B, ..., F
W_N, W_M, W_L, Pedostructure water content (kg kg^{-1}) at Points N, M, L
V_A, V_B, ..., V_F, Pedostructure specific volume (dm^3 kg^{-1}) at Points A, B, ..., F
V_N, V_M, V_L, Pedostructure specific volume (dm^3 kg^{-1}) at Points N, M, L
$V_{N'}$, $V_{M'}$, $V_{L'}$, y-axis values (dm^3 kg^{-1}) of Points N′, M′, L′ in the SC graph
K_{rs}, K_{bs}, K_{ss}, K_{ip}, Slopes of the SC linear phases (dm^3 kg^{-1})
k_N, k_M, k_L, Shape parameters (kg kg^{-1}) of the SC equation

APPENDIX 2

Equations of the Exponential Model

Points A, B, C, ..., and F were defined as the parameters of the exponential equation (XP model) that fits the curvilinear phases of the SC. For example, the expression for the curvilinear Phase D–C is:

$$V = V_D + \frac{(W_C - W_D)}{e - 1}\{k_{bs}[\exp(W_n) - W_n - 1] + K_{st}[eW_n - \exp(W_n) + 1]\} \quad [A1]$$

where $W_n = (W - W_D)/(W_C - W_D)$ and e = exp(1) = 2.718.

This leads to the important relationships between parameters when $W = W_C$ in Eq [A1]:

$$(V_C - V_D)/(W_C - W_D) = [K_{bs}(e - 2) + K_{st}]/(e - 1) \approx 0.418\, K_{bs} \quad [A2]$$

This last equation is used to establish the relationships in Table 3.

APPENDIX 3

Significance of the Parameters k_J and W_J, (J = N, M, and L)

Equations for the tangents at the linear phases represented by Points I_{re}, I_{bs}, I_{st}, and I_{ip} in Fig. 3 are obtained by integrating Eq. [1] (see main text) into each Segment L, M, and N of the curve. For the Segment M of the SC, integration of Eq. [1] and [9] according to [7] gives:

$$V - V_M = K_{bs}(w_{bs} - w_{bsM}) + K_{st}(w_{st} - w_{stM})$$

$$V - V_M = \frac{K_{bs}}{k_M}\mathrm{Log}\left\{\frac{1 + \exp[k_M(W - W_M)]}{2}\right\} - \frac{K_{st}}{k_M}\mathrm{Log}\left\{\frac{1 + \exp[-k_M(W - W_M)]}{2}\right\} \quad [A3]$$

Equations for the tangents are:

$$V - V_M = -\frac{(K_{bs} - K_{st})}{k_M}\mathrm{Log}2 - K_{st}(W - W_M) \text{ for } W \gg W_M \quad [A4]$$

(in the linear structural shrinkage phase), and in the linear basic shrinkage phase:

$$V - V_M = -\frac{(K_{bs} - K_{st})}{k_M}\mathrm{Log}2 + K_{bs}(W - W_M) \text{ for } W \ll W_M \quad [A5]$$

Thus, the coordinates of the intersection Point M′ of the two lines are:

$$W_{M'} = W_M \text{ and } V_{M'} = V_M - (K_{bs} - K_{st})\,\mathrm{Log}2/k_M \quad [A6]$$

The intersection Point M′ and the Point *M* of the SC have the same *x*-coordinate and k_M represents the reverse of the distance MM′ except for the factor $(K_{bs} - K_{st})$ Log2. The same reasoning applies for Parts L and N of the SC that gives:

$$W_{L'} = W_L \text{ and } V_{L'} = V_L - (K_{ip} - K_{st})\mathrm{Log}2/k_L \quad [A7]$$

$$W_{N'} = W_N \text{ and } V_{N'} = V_N - (K_{bs} - K_{re})\mathrm{Log}2/k_N \quad [A8]$$

These three last equations are listed in Table 3 and are used to transform the PS parameters into XP parameters.

The SL Method for the XP and PS Models, and the Required Parameters

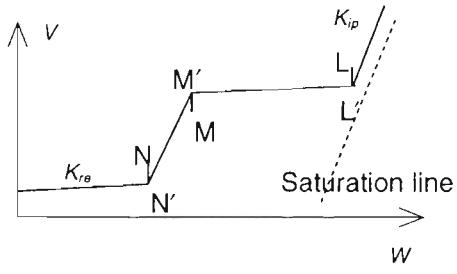

Building the SC according the XP and using the SL method proposed by Braudeau et al. (1999) needs, as for the current PS model, the four tangent lines at the inflexion points of the SC (eight parameters), plus the *y* axis of the three points, N, M, and L, (three parameters) of the SC corresponding to the intersection points N′, M′, and L′ of the tangents. This leads to 11 parameters. If the enclosed porosity (nonconnected) is neglected, then the interpedal shrinkage line (IP-line) is identified to as the saturation line of which the slope is unity and the necessary parameters number becomes 10. In that case, $W_{sat} = W_L$ and $V_s = V_L - W_L$.

Thus, if there are no other pore subsystem in the pedostructure other than the primary peds and their assembly, the two slopes at the extremes of the curve reduce to zero for $W = 0$ and one for $W \gg W_{sat}$. Therefore, the pedostructure description space is nine-dimensional if the enclosed porosity is neglected (IP-line and saturation line are merged).

In most cases, simplifications can be made: $K_{re} = 0$; $K_{st} = 0$; $V_s = 0.4$ ($d_s = 2.5$ kg dm^{-3}), which reduces the parameters number. Additionally, if the interpedal shrinkage is also neglected (for modeling soil in situ, for example) the five-phases SC is considered with only six parameters required, such as:

$$V_o = V_{N'};\ V_D = V_{M'};\ W_N;\ W_{M'};\ k_N;\ k_M$$

or

$$V_o = V_A;\ W_A;\ W_B;\ W_C;\ W_D;\ K_{bs}$$

V_B and V_D being calculated using (Eq. [A2]).

ACKNOWLEDGMENTS

This work was partially conducted while two of the authors were on leave at Cirad in the COTONS Decision Support team. The authors thank the support and the encouragement provided by IRD, CIHEAM-IAMM, Cirad, and Purdue University.

REFERENCES

Braudeau, E. 1988a. Equation généralisée des courbes de retrait d'échantillons de sol structurés. (In French.) C.R. Acad. Sci. Paris 307:1731–1734.

Braudeau, E. 1988b. Essai de caractérisation quantitative de l'état structural d'un sol basé sur l'étude de la courbe de retrait. (In French.) C.R. Acad. Sci. Paris 307:1933–1936.

Braudeau, E., and A. Bruand. 1993. Détermination de la courbe de retrait de la phase argileuse à partir de la courbe de retrait établie

sur échantillon de sol non remanié. (In French.) C.R. Acad. Sci. Paris. 316:685–692.
Braudeau, E., J.M. Costantini, G. Bellier, and H. Colleuille. 1999. New device and method for soil shrinkage curve measurement and characterization. Soil Sci. Soc. Am. J. 63:525–535.
Braudeau, E., C. Zidi, A. Loukil, C. Derouiche, D. Decluseau, M. Hachicha, and A. Mtimet. 2001. Un système d'information pédologique, le SIRS-Sols du périmètre irrigué de Cébala-Borj-Touil. (Basse Vallée de la Majerda). Bulletin Sols de Tunisie, numéro spécial 2001. Direction des sols (Ed.), Tunis, Tunisia.
Brewer, R. 1964. Fabric and Mineral Analysis of Soils. John Wiley & Sons, New York.
Chertkov, V.Y. 2000. Modelling the pore structure and shrinkage curve of soil clay matrix. Geoderma 95:215–246.
Colleuille, H., and E. Braudeau. 1996. A soil fractionation related to soil structural behavior. Aust. J. Soil Res. 34:653–669.
Coppola, A. 2000. Unimodal and bimodal description of hydraulic properties for aggregated soils. Soil Sci. Soc. of Am. J. 64:1252–1262.
Giraldez, J.V., G. Sposito, and C. Delgado. 1983. A general soil volume change equation. I. The two parameter model. Soil Sci. Soc. Am. J. 47:419–422.
Groenevelt, P.H., and G.H. Bolt. 1972. Water retention in soil. Soil Sci. 113:238–245.
Groenevelt, P.H., and C.D. Grant. 2001. Re-evaluation of the structural properties of some British swelling soils. Eur. J. Soil Sci. 52: 469–477.
McGarry, D., and K.W.J. Malafant. 1987. The analysis of volume change in unconfined units of soil. Soil Sci. Soc. Am. J. 51:290–297.
Perrier, E., C. Mullon, M. Rieu, and G. de Marsily. 1995. Computer construction of soil structures: Simulation of their hydraulic and shrinkage properties. Water Resour. Res. 31:2927–2943.
Sposito, G. 1973. Volume changes in swelling clays. Soil Sci. 115: 315–320.
Sposito, G., and J.V. Giraldez. 1976. Thermodynamic stability and the law of corresponding states in swelling soils. Soil Sci. Soc. Am. J. 40:352–358.
Tariq, A.U.R., and D.S. Durnford. 1993. Analytical volume change for model for swelling clay soils. Soil Sci. Soc. Am. J. 57:1183–1187.
Voltz, M., and Y.M. Cabidoche. 1995. Non-uniform volume and water content changes in swelling clay soil. Theoretical analysis. Eur. J. Soil Sci. 46:333–343.
Yong, R.N., and B.P. Warkentin. 1966. Introduction to soil behavior. The MacMillan Co., New York.
Zidi, C., and E. Braudeau. 1998. Le rétractomètre: Mode d'emploi et utilisation pour la caractérisation hydrostructurale des sols. (In French.) Études Spéciales ES no 303. Direction des Sols. Ministère de l'Agriculture, Tunis, Tunisia.